Anal. Chem. **1996,** *68,* 271−280

Correction of Mass Spectral Drift Using Artificial Neural Networks

Royston Goodacre* and Douglas B. Kell†

Institute of Biological Sciences, University of Wales, Aberystwyth, Dyfed SY23 3DA, Wales, U.K.

For pyrolysis mass spectrometry (PyMS) to be used for the routine identification of microorganisms, for quantifying determinands in biological and biotechnological systems, and in the production of useful mass spectral libraries, it is paramount that newly acquired spectra be compared to those previously collected. Neural network and other multivariate calibration models have been used to relate mass spectra to the biological features of interest. As commonly observed, however, mass spectral fingerprints showed a lack of long-term reproducibility, due to instrumental drift in the mass spectrometer; when identical materials were analyzed by PyMS at dates from 4 to 20 months apart, neural network models produced at *earlier* times could not be used to give accurate estimates of determinand concentrations or bacterial identities. Neural networks, however, can be used to correct for pyrolysis mass spectrometer instrumental drift *itself*, so that neural network or other multivariate calibration models created using previously collected data can be used to give accurate estimates of determinand concentration or the nature of bacteria (or, indeed, other materials) from newly acquired pyrolysis mass spectra. This approach is not limited solely to pyrolysis mass spectrometry but is generally applicable to any analytical tool which is prone to instrumental drift, such as IR, ESR, NMR and other spectroscopies, and gas and liquid chromatography, as well as other types of mass spectrometry.

There is a continuing need for more rapid, precise, and accurate analyzes of the (bio)chemical composition of (micro)-biological systems, both within biotechnology and for the identification of potentially pathogenic organisms. An ideal method would require minimum sample preparation, would analyze samples directly (i.e., be reagentless), and would be rapid, automated, quantitative, and (at least relatively) inexpensive. Pyrolysis mass spectrometry (PyMS) is an instrument-based technique which satisfies these requirements.

Pyrolysis is the thermal degradation of complex material in an inert atmosphere or a vacuum which causes molecules to cleave at their weakest points to produce smaller, volatile fragments. Curie-point pyrolysis is a particularly reproducible and straightforward version of the technique, in which the sample, dried onto an appropriate metal, is rapidly heated (0.5 s is typical) to the Curie point of the metal. These degradation products are then separated and counted by a mass spectrometer so as to produce a pyrolysis mass spectrum (150 m/z intensities; from m/z 51 to 200), which can then be used as a "chemical profile" or fingerprint of the complex material analyzed.[1,2]

PyMS is a highly discriminatory method,[3] which is applicable to any organic material.[1,4] The technique is well established within (micro)biology for the differentiation and identification of groups of bacteria, fungi, and yeasts.[1,4−6] and has also been applied to the authentication of foodstuffs.[7−11]

Recently, the PyMS technique has been expanded within our laboratory for the *quantitative* analysis of the chemical constituents of microbial and other samples, via the application of the novel *supervised* learning methods of artificial neural networks (ANNs) (see refs 12−25 for introductory surveys) and the multivariate linear regression techniques of partial least-squares regression (PLS) and principal components regression (PCR) (see refs 26−

* Address correspondence to this author. E-mail: rgg@aber.ac.uk and http://gepasi.dbs.aber.ac.uk/roy/pymshome.htm.

† E-mail: dbk@aber.ac.uk.

(1) Meuzelaar, H. L. C.; Haverkamp, J.; Hileman, F. D. *Pyrolysis Mass Spectrometry of Recent and Fossil Biomaterials*; Elsevier: Amsterdam, 1982.
(2) Irwin, W. J. *Analytical Pyrolysis: A Comprehensive Guide*; Marcel Dekker: New York, 1982.
(3) Goodacre, R.; Berkeley, R. C. W. *FEMS Microbiol. Lett.* ***1990***, *71*, 133−138.
(4) Goodacre, R. *Microbiol. Eur.* **1994**, *2* (2), 16−22.
(5) Gutteridge, C. S. *Methods Microbiol.* **1987**, *19*, 227−272.
(6) Magee, J. T. In *Handbook of New Bacterial Systematics*; Goodfellow, M., O'Donnell, A. G., Eds.; Academic Press: London, 1993; pp 383−427.
(7) Aries, R. E.; Gutteridge C. S.; Evans, R. *J. Food Sci.* **1986**, *51*, 1183−1186.
(8) Goodacre, R.; Kell, D. B.; Bianchi, G. *Nature* **1992**, *359*, 594.
(9) Goodacre, R.; Kell, D. B.; Bianchi, G. *J. Sci. Food Agric.* **1993**, *63*, 297−307.
(10) Reid, K. J. G.; Swan, J. S.; Gutteridge, C. S. *J. Anal. Appl. Pyrol.* **1993**, *25*, 49−62.
(11) Aylott, R. I.; Clyne, A. H.; Fox, A. P.; Walker, D. *Analyst* **1994**, *119*, 1741−1746.
(12) Rumelhart, D. E.; McClelland, J. L.; PDP Research Group. *Parallel Distributed Processing. Experiments in the Microstructure of Cognition*; MIT Press: Cambridge, MA, 1986; Vols. I & II.
(13) Beale, R.; Jackson, T. *Neural Computing: An Introduction*; Adam Hilger: Bristol, 1990.
(14) Eberhart, R. C.; Dobbins, R. W. *Neural Network PC Tools*; Academic Press: London, 1990.
(15) Pao, Y.-H. *Adaptive Pattern Recognition and Neural Networks*; Addison-Wesley: Reading, MA, 1989.
(16) Wasserman, P. D. *Neural Computing: Theory and Practice*; Van Nostrand Reinhold: New York, 1989.
(17) Wasserman, P. D.; Oetzel, R. M. *NeuralSource: the Bibliographic Guide to Artificial Neural Networks*; Van Nostrand Reinhold: New York, 1989.
(18) Simpson, P. K. *Artificial Neural Systems*; Pergamon Press: Oxford, 1990.
(19) Hecht-Nielson, R. *Neurocomputing*; Addison-Wesley: Reading, MA, 1990.
(20) Hertz, J.; Krogh, A.; Palmer, R. G. *Introduction to the Theory of Neural Computation*; Addison-Wesley: Redwood City, CA, 1991.
(21) Peretto, P. *An Introduction to the Modelling of Neural Networks*; Cambridge University Press: Cambridge, 1992.
(22) Gallant, S. I. *Neural Network Learning*; MIT Press: Cambridge, MA, 1993.
(23) Næs, T.; Kvaal, K.; Isaksson, T.; Miller, C. *J. Near Infrared Spectrosc.* **1993**, *1*, 1−11.
(24) Zupan, J.; Gasteiger, J. *Neural Networks for Chemists: An Introduction*; VCH Verlagsgeesellschaft: Weinheim, 1993.
(25) Goodacre, R.; Neal, M. J.; Kell, D. B. *Zentralbl. Bakteriol. Mikrobiol., Reihe C*, in press.

0003-2700/96/0368-0271$12.00/0

35 for first-rate texts). For example, we have shown that it is possible using this method to follow the production of indole in a number of strains of *E. coli* grown on media incorporating various amounts of tryptophan,[36] to quantify the (bio)chemical constituents of complex biochemical binary mixtures of proteins and nucleic acids in glycogen,[37,38] and to measure the concentrations of tertiary mixtures of cells of the bacteria *Bacillus subtilis*, *Escherichia coli*, and *Staphylococcus aureus*.[38] For biotechnological purposes, the powerful combination of PyMS and ANNs has been used for the quantitative analysis of recombinant cytochrome b_5 expression in *E. coli*,[39] and for effecting the rapid screening for the high-level production of desired substances in fermentor broths.[40,41]

With regard to classifications and discriminations, PyMS and ANNs have also been exploited for the rapid and accurate assessment of the presence of lower-grade seed oils as adulterants in extra-virgin olive oils,[8,9] and to effect the rapid identification of strains of *E. coli*,[42] *Eubacterium*,[43] *Mycobacterium*,[44] *Propionibacterium* spp.,[45] and *Streptomyces*.[46] This approach is far more attractive for the identification of samples from their pyrolysis mass spectra since it no longer involves the interpretation of complex principal components analysis and canonical variates analysis plots because the identities are binary-encoded at the output layer of the neural network, and so the results are easily read.

Within clinical microbiology, because of the uncertainties over the long-term reproducibility of the PyMS system, PyMS has really been limited to the typing of short-term outbreaks, where all microorganisms are analyzed in a single batch.[47−49] In a study to differentiate between different strains of *Carnobacterium*,[50] the short-term reproducibility over a period of 4 weeks was excellent; the separation of the five type strain species examined was sustained, and the spectra had not changed significantly over the 4 weeks. Shute et al.[51] also investigated the reproducibility of the PyMS system over a much longer period of 14 months for differentiating some *Bacillus* species. Although these bacteria were classified similarly at the beginning and end of the time period, direct comparison of the two data sets was not possible. Curie-point pyrolysis is very reproducible, and the pyrolysate transfer to the ion source of the mass spectrometer is also tightly controlled; therefore, the major contribution to long-term irreproducibility is ion source aging (over long periods of extended use, intractable organic debris collects around the ion source), which alters the transmissivity of ions, thus causing mass spectral drift. In a recent study to characterize the origin of green coffee,[52] it was concluded that PyMS would not be satisfactory until an improvement in reproducibility was found, since reliable differentiation was not obtained.

For PyMS to be (a) used for the routine identification of microorganisms and (b) combined with ANNs to quantify biological systems (e.g., metabolites of interest in fermentor broths), new spectra must be able to be compared to those previously collected.

The first strategy to compensate (correct) for mass spectral drift is to tune the instrument. For mass spectrometry, this is typically achieved using the volatile standard perfluorokerosene and tuning, within the m/z 51−200 range, such that m/z 181 was one-tenth of m/z 69. Unfortunately, this procedure does not compensate for all the instrumental drift, and additional methods need to be sought.

To correct for drift, one would need to analyze the *same* standards at the two different times and use some sort of mathematical correction method. This could simply be subtracting the amount of drift from new spectra collected; however, this assumes that the drift is uniform (linear) with time, which is obviously not the case. This method also relies on the variables (masses) being void of noise, which is also not the case with (pyrolysis) mass spectral data. An alternative method would be to *transform* the mass spectra to look like the mass spectra of the same material previously collected using a method which was (a) robust to noisy data and (b) able to perform nonlinear mappings. Artificial neural networks carry out nonlinear mappings while still being able to map the linearities and are purported to be robust to noisy data. These mathematical methods are therefore ideally suited to be exploited for the correction of mass spectral drift.

Smits et al.[53] have implemented a drift correction for pattern recognition using neural networks using *simulated* flow cytometry data. These data sets contained only two variables, and the amount of drift was included in neural networks as an *extra* input variable (three input nodes in total). It is, however, often difficult to measure the amount of drift accurately in real systems, especially if the number of input variables is high (typically 150 with pyrolysis mass spectral data); a better method would be to *transform* the spectra collected today to be like those collected previously.

In the present study, we therefore reanalyzed four systems using PyMS which had previously been studied and reported in the literature. The duplicate data sets spanned time periods between 4 and 20 months and included (1) the quantification of

(26) Joreskog, K.; Wold, H. *Systems under direct observation*; North Holland: Amsterdam, 1982
(27) Haaland, D. M.; Thomas, E. V. *Anal. Chem.* **1988**, *60*, 1193−1202.
(28) Manne, R. *Chemom. Intell. Lab. Syst.* **1987**, *2*, 187−197.
(29) Martens H.; Næs, T. *Multivariate Calibration*; John Wiley and Sons: New York, 1989.
(30) Malinowski, E. R. *Factor Analysis in Chemistry*; John Wiley & Sons: New York, 1991.
(31) Brereton, R. G. *Multivariate Pattern Recognition in Chemometrics*; Elsievier: Amsterdam, 1992.
(32) McAvoy,T. J.; Su, H. T.; Wang, N. S.; He, M. *Biotechnol. Bioeng.* **1992**, *40*, 53−62.
(33) Martin, K. A. *Appl. Spectrosc. Rev.* **1992**, *27*, 325−383.
(34) Frank, I. E.; Friedman, J. H. *Technometrics* **1993**, *35*, 109−135.
(35) Liang, Y.-Z.; Kvalheim, O. M.; Manne, R. *Chemom. Intell. Lab. Syst.* **1993**, *18*, 235−250.
(36) Goodacre, R.; Kell, D. B. *Anal. Chim. Acta* **1993**, *279*, 17−26.
(37) Goodacre, R.; Edmonds A. N.; Kell, D. B. *J. Anal. Appl. Pyrol.* **1993a**, *26*, 93−114.
(38) Goodacre, R.; Neal, M. J.; Kell, D. B. *Anal. Chem.* **1994**, *66*, 1070−1085.
(39) Goodacre, R.; Karim, A.; Kaderbhai, M.; Kell, D. B. *J. Biotechnol.* **1994**, *34*, 185−193.
(40) Goodacre, R.; Trew, S.; Wrigley-Jones, C.; Neal, M. J.; Maddock, J.; Ottley, T. W.; Porter, N.; Kell, D. B. *Biotechnol. Bioeng.* **1994**, *44*, 1205−1216.
(41) Goodacre, R.; Trew, S.; Wrigley-Jones, C.; Saunders, G.; Neal, M. J.; Porter, N.; Kell, D. B. *Anal. Chim. Acta* **1995**, *313*, 25−43.
(42) Sisson, P. R.; Freeman, R.; Law, D.; Ward, A. C.; Lightfoot, N. F. *J. Anal. Appl. Pyrol.* **1995**, *32*, 179−185.
(43) Goodacre, R.; Hiom, S.; Cheeseman, S. L.; Murdoch, D.; Weightman, A. J.; Wade, W. G. *Curr. Microbiol.*, in press.
(44) Freeman, R.; Goodacre, R.; Sisson, P. R.; Magee, J. G.; Ward, A. C.; Lightfoot, N. F. *J. Med. Microbiol.* **1994**, *40*, 170−173.
(45) Goodacre, R.; Neal, M. J.; Kell, D. B.; Greenham, L. W.; Noble, W. C.; Harvey, R. G. *J. Appl. Bacteriol.* **1994**, *76*, 124−134.
(46) Chun, J.; Atalan, E.; Ward, A.C.; Goodfellow, M. *FEMS Microbiol. Lett.* **1993**, *107*, 321−325.
(47) Freeman, R.; Goodfellow, M.; Gould, F. K.; Hudson, S. J.; Lightfoot, N. F. *J. Med. Microbiol.* **1990**, *32*, 283−286.
(48) Sisson, P. R.; Freeman, R.; Lightfoot, N. F.; Richardson, I. R. *Epidemiol. Infect.* **1991**, *107*, 127−132.
(49) Magee, J. T.; Hindmarch, J. M.; Burnett, I. A.; Pease, A. *J. Med. Microbiol.* **1989**, *30*, 273−278.
(50) Manchester, L. N.; Toole, A.; Goodacre, R. *J. Appl. Bacteriol.* **1995**, *78*, 88−96.
(51) Shute, L. A.; Gutteridge, C. S.; Norris, J. R.; Berkeley, R. C. W. *J. Appl. Bacteriol.* **1988**, *64*, 79−88.
(52) Krivan, V.; Barth, P.; Morales, A. F. *Mikrochim. Acta* **1993**, *110*, 217−236.
(53) Smits, J. R. M.; Melssen, W. J.; Derksen, M. W. J.; Kateman G. *Anal. Chim. Acta* **1993**, *284*, 91−105.

lysozyme in glycogen,[38] (2) the quantification of *S. aureus* in *E. coli*,[25,38] (3) the quantification of the antibiotic ampicillin in *E. coli*[40] to mimic a fermentor, and (4) the identification of human isolates of *Propionibacterium acnes*.[54] We applied neural networks, with (150-8-150) or without (150-150) a hidden layer, to correct for mass spectral drift by transforming data collected now into mass spectra previously collected and compared the results with correction techniques which exploited linear transformations either by subtracting the drift or by using a mass-by-mass linear scalar based on the ratio of the old to new mass values. This work has been described in a patent application.[55]

EXPERIMENTAL SECTION

Pyrolysis Mass Spectrometry. Five microliter aliquots of the samples (see below for details of the four data sets) were evenly applied onto iron−nickel foils. Prior to pyrolysis, the samples were oven-dried at 50 °C for 30 min. Samples were run in triplicate. The pyrolysis mass spectrometer used was the Horizon Instruments PYMS-200X (Horizon Instruments Ltd., Heathfield, U.K.) as initially described by Aries et al.[56] For full operational procedures, see Goodacre et al.[38,40,45] The sample tube carrying the foil was heated, prior to pyrolysis, at 100 °C for 5 s. Curie-point pyrolysis was at 530 °C for 3 s, with a temperature rise time of 0.5 s. These conditions were used for all experiments.

The pyrolysis mass spectra that were collected were normalized so that the total ion count was 2^{16} to remove the influence of sample size per se.

Prior to any analysis, the mass spectrometer was calibrated using the chemical standard perfluorokerosene (Aldrich), such that *m/z* 181 was one-tenth of *m/z* 69.

Principal Components Analysis. The data from PyMS may be displayed as quantitative pyrolysis mass spectra (e.g., as in Figure 1, normalized here to percentage ion count). The abscissa represents the *m/z* ratio, while the ordinate contains information on the ion count for any particular *m/z* value ranging from 51 to 200.

To observe the *natural* relationships between samples, the normalized data were then analyzed by principal components analysis (PCA[57−61] using the program Unscrambler II Version 4.0 (CAMO A/S, Trondheim, Norway), which runs under Microsoft MS-DOS 6.2 on an IBM-compatible PC. PCA is a well-known technique for reducing the dimensionality of multivariate data while preserving most of the variance, and while it does not take account of any groupings in the data, neither does it require that the populations be normally distributed, i.e., it is a nonparametric method.

Artificial Neural Networks. All ANN analyzes were carried out using a user-friendly, neural network simulation program,

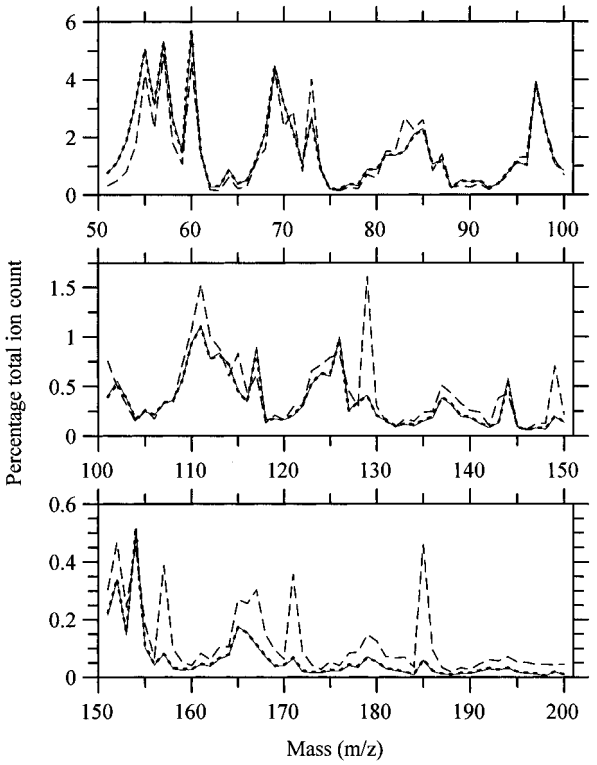

Figure 1. Normalized pyrolysis mass spectra of 35 μg of lysozyme mixed with 20 μg of glycogen, analyzed on 27 Aug, 1992 (—), 19 April, 1994 (– –), and the spectra from 19 April, 1994, after drift correction by a 150-8-150 neural network trained to transform data collected at time 2 into data collected at time 1 (- - -).

NeuralDesk (Neural Computer Sciences, Southampton, U.K.), which runs under Microsoft Windows 3.1 on an IBM-compatible PC. To ensure maximum speed, an accelerator board for the PC (NeuSprint) based on the AT&T DSP32C chip, which effects a speed enhancement of some 100-fold compared with a 386 PC, permitting the analysis (and updating) of some 400 000 weights per second, was used. Data were also processed prior to analysis using the Microsoft Excel 4.0 spreadsheet.

The algorithm used was standard back-propagation,[12,62] which employs processing nodes (neurons or units), connected using abstract interconnections (connections or synapses). Connections each have an associated real value, termed the weight, that scales signals passing through them. Nodes sum the signals feeding to them and output this sum to each driven connection scaled by a "squashing" function (*f*) with a sigmoidal shape, typically the function $f = 1/(1 + e^{-x})$, where $x = \sum$inputs.

For the training of the ANN, each input (i.e., normalized pyrolysis mass spectrum) is paired with a desired output (see below for output pattern); together these are called a training pair (or training pattern). An ANN is trained over a number of training pairs; this group is collectively called the training set. The input is applied to the network, which is allowed to run until an output is produced at each output node. The differences between the actual and the desired output, taken over the entire training set, are fed back through the network in the reverse direction to signal flow (hence back-propagation), modifying the weights as they go. This process is repeated until a suitable level of error is achieved. In the present work, we used a learning rate of 0.1 and a

(54) Goodacre, R.; Howell, S. A.; Noble, W. C.; Neal, M. J. *Zentralbl. Bakteriol. Mikrobiol., Reihe C*, in press.
(55) Goodacre, R.; Kell, D. B. U.K. Patent #9511619.0, 1995.
(56) Aries, R. E.; Gutteridge, C. S.; Ottley, T. W. *J. Anal. Appl. Pyrol.* **1986**, *9*, 81−98.
(57) Chatfield, C.; Collins, A. J. *Introduction to Multivariate Analysis*; Chapman & Hall: London, 1980; pp 57−81.
(58) Causton, D. R. *A Biologist's Advanced Mathematics*; Allen & Unwin: London, 1987; pp 48−72.
(59) Gutteridge, C. S.; Vallis, L.; MacFie, H. J. H. In *Computer-assisted Bacterial Systematics*; Goodfellow, M., Jones, D., Priest, F. G., Eds.; Academic Press: London, 1985; pp 369−401.
(60) Flury, B.; Riedwyl, H. *Multivariate Statistics: A Practical Approach*; Chapman & Hall: London, 1988; pp 181−233.
(61) Everitt, B. S. *Cluster Analysis*; Edward Arnold: London, 1993.
(62) Werbos, P. J. *The Roots of Back-Propagation: From Ordered Derivatives to Neural Networks and Political Forecasting*; John Wiley & Sons: Chichester, 1993.

Table 1. Time Table of the Four Duplicate PyMS Experiments Studied To Investigate Instrumental Drift

purpose of PyMS experiment	ref	pyrolysis mass spectra collected		time difference	
		time 1	time 2	days	months
quantify lysozyme in glycogen	38	27 Aug, 1992	19 Apr, 1994	600	19.7
quantify *S. aureus* in *E. coli*	25, 38	30 Sept, 1992	18 Apr, 1994	535	17.6
quantify ampicillin in *E. coli*	40	22 July, 1993	19 Apr, 1994	271	8.9
identify *P. acnes* human isolates	54	28 Jan, 1994	2 June, 1994	125	4.1

momentum of 0.9. Learning rate scales the magnitude of the step down the error surface taken after each complete calculation in the network (epoch), and momentum acts like a low-pass filter, smoothing out progress over small bumps in the error surface by remembering the previous weight change.

The structure of the ANNs used in this study consisted of an input layer comprising 150 nodes (normalized pyrolysis mass spectra) connected to the output layer containing x nodes (where x is the number of determinands) via a single "hidden" layer containing 8 nodes; for some analyzes, the hidden layer was not used. The topology containing a hidden layer may be represented as a 150-8-x architecture. In addition, the hidden layer (if present) and output layer were connected to the bias (the activation of which is always +1), whose weights will also be altered during training. Before training commenced, the values applied to the input and output nodes were normalized between 0 and +1, and the connection weights were set to small random values.[16]

Preparation of Samples for the Investigation into Mass Spectral Drift. Four data sets were analyzed at two different times. The work was originally conducted (and later published) at time 1, and the samples were reanalyzed under nominally identical conditions at time 2. The details of when these four data sets were collected and the various time differences are given in Table 1.

Quantification of Lysozyme in Glycogen Data Set. The mixtures were prepared such that 5 mL of a solution contained 0−100 mg (in steps of 5 mg) of lysozyme (from chicken egg white, Sigma) in 20 mg of glycogen (oyster type II, Sigma).[38]

To quantify the amount of lysozyme mixed in glycogen a 150-8-1 ANN was trained, as detailed in Table 2 and previously described by Goodacre et al.,[38] with data from the mass spectra collected on 27 August, 1992 (time 1).

Quantification of Ampicillin in *E. coli* Data Set. Ampicillin (desiccated D-(−)-α-aminobenzylpenicillin sodium salt, ≥98% (titration), Sigma) was prepared in bacterial slurries of 40 mg mL^{-1} *E. coli* W3110 (as prepared below) to give a concentration range of 0−5000 μg mL^{-1} in 250 μg mL^{-1} steps.[40]

To quantify the amount of ampicillin in *E. coli*, a 150-8-1 ANN was trained, as detailed in Table 2 and previously described by Goodacre et al.,[40] with data from the mass spectra collected on 22 July, 1993 (time 1).

Quantification of *S. aureus* in *E. coli* Data Set. The bacteria used were *E. coli* W3110 and *S. aureus* NCTC6571. Both strains were grown in 2 L of liquid media (glucose (BDH), 10.0 g; peptone (LabM), 5.0 g; beef extract (LabM), 3.0 g; H_2O, 1 L) for 16 h at 37 °C in a shaker. After growth, the cultures were harvested by centrifugation and washed in phosphate-buffered saline (PBS). The dry weights of the cells were estimated gravimetrically and used to adjust the weight of the final slurries using PBS to approximately 40 mg mL^{-1}. Mixtures were then prepared that consisted of *x*% *E. coli* and *y*% *S. aureus*, where *x*:*y* were 100:0, 90:80, 80:20, 75:25, 70:30, 60:40, 50:50, 40:60, 30:70, 25:75, 20:80, 10:90, and 0:100.[25,38]

To quantify the amount of *S. aureus* mixed with *E. coli*, a 150-8-1 ANN was trained, as detailed in Table 2 and previously described by Goodacre et al.,[25] with data from the mass spectra collected on 30 September, 1992 (time 1).

Identification of *P. acnes* Data Set. *P. acnes* isolates were recovered from the foreheads of three normal adults.[54] Nine isolates were taken from person a, five from person b, and five from person c. The *P. acnes* isolates were incubated anaerobically for 7 days at 37 °C on a single batch of coryneform agar (CA; composition (in g L^{-1}) tryptone soya broth (Oxoid), 30; yeast extract (Oxoid), 10; agar No. 1 (Oxoid), 10; and Tween 80 (Sigma), 10 mL L^{-1}). After growth, biomass was carefully collected in PBS and frozen at −20 °C.

To identify the *P. acnes* a 150-8-3 ANN was trained with data from the mass spectra collected on 28 January, 1994 (time 1). The training input data were the replicate normalized pyrolysis mass spectra of two isolates from each of the people (and see Table 4), and the outputs were binary encoded such that *P. acnes* from person a were coded as 100, thosee from person b as 010, and those from person c as 001. The input layer was scaled across the whole mass range from 0 to 3500; the output layer was scaled between 0 and 1. Training was stopped when the %RMS error in the training set was 1%; this took approximately 2×10^3 epochs.

Drift Correction. Four methods of drift correction were employed to transform pyrolysis mass spectra collected at time 2 into those collected previously at time 1. This procedure should then allow new mass spectra to be directly compared with old mass spectra and used to challenge neural networks previously trained with data from time 1, to quantify or identify the various biological systems described above.

Calibration spectra were chosen at the two time periods: (1) for the quantification of lysozyme in glycogen, these were the replicate normalized pyrolysis mass spectra containing 0, 25, 50, 75, and 100 μg of lysozyme in 20 μg of glycogen; (2) for the calculation of the ampicillin titer in *E. coli*, these were the replicate normalized pyrolysis mass spectra containing 0, 1250, 2500, 3750, and 5000 μg mL^{-1} ampicillin in 40 mg mL^{-1} *E. coli*; (3) for the quantification of *S. aureus* mixed with *E. coli*, these were the replicate normalized pyrolysis mass spectra containing 0, 25, 50, 75, and 100% *S. aureus;* finally (4) for the identification of *P. acnes*, these were the triplicate mass spectra from two isolates from each of the three people.

The first neural network-based method to correct for drift employed 150-8-150 ANNs; the input to the network comprised the normalized pyrolysis mass spectra from the calibration samples collected at time 2, and the output layer comprised the mass spectra of the same calibration material analyzed at time 1. Neural networks were also used which contained no hidden layer (this is represented as a 150-150 ANN). Both types of neural networks employed the back-propagation algorithm; the input and output layers were scaled to lie between 0 and +1 across the 51−200 mass range and trained until an average RMS error of 0.5% was reached. Given the large number of connection weights to be updated, 2558 weights for 150-8-150 ANNs and 22 650 weights

Table 2. Optimal Neural Network Solutions Used for Quantification of the Three Systems from Their Pyrolysis Mass Spectra Analyzed at Time 1 (Table 1)

	lysozyme (μg) in 20 μg of glycogen[38],[a]	ampicillin titer (μg mL^{-1}) in 40 mg mL^{-1} *E. coli*[40],[a]	*S. aureus* in *E. coli* (%)[25,a]
training data	0, 10, 20, 30, 40, 50, 60, 70, 80, 90, 100	0, 500, 1000, 1500, 2000, 2500, 3000, 3500, 4000, 4500, 5000	0, 25, 50, 75, 100
cross-validation data	5, 15, 25, 35, 45, 55, 65, 75, 85, 95	250, 750, 1250, 1750, 2250, 2750, 3250, 3750, 4250, 4750	10, 20, 30, 40, 60, 70, 80, 90
scaling on			
input layer[b]	0−5000	0−5000	0−6000
output layer	-50−150	-2500−7500	-10−110
%RMS error			
training set	0.5	1.0	0.3
cross-validation set	1.36	1.14	1.55
No. of epochs	1×10^4	2×10^3	5×10^3

[a] The best generalization point was established using cross-validation and was previously found and published elsewhere. [b] Input layer was scaled across the whole mass range.

for 150-150 ANNs, this was relatively quick and typically took between 2×10^3 and 1×10^4 epochs.

To compare the performance of these two neural network-based drift corrections with that of corrections based on linear corrections alone, two methods relying on mass-by-mass transformations were also studied. Linear subtractions were used where the amount of drift in each mass was calculated by first subtracting the normalized mass spectrum collected at time 1 (old) from the mass spectrum collected at time 2 (new); this was done for the calibration samples and the average drift in each mass computed. These drift correction values were then subtracted from each of the masses in newly acquired (time 2) mass spectra:

$$\text{linear method 1} = (\text{new mass}) - [\text{average of } (\text{new calibration mass} - \text{old calibration mass})]$$

The second linear transformation involved calculating the average mass-by-mass ratio between the mass spectra of the calibration samples collected at time 1 (old) and time 2 (new). These ratios were then used to scale each of the masses in newly acquired mass spectra collected at time 2:

$$\text{linear method 2} = (\text{new mass})[\text{average ratio of } (\text{old calibration mass}/\text{new calibration mass})]$$

RESULTS AND DISCUSSION

Drift Correction. (i) Quantification of Lysozyme in Glycogen. Pyrolysis mass spectral fingerprints of 35 μg of lysozyme mixed with 20 μg of glycogen analyzed at time 1 on 27 August, 1992 and the same material analyzed 600 days later on 19 April, 1994 (time 2) are shown in Figure 1. These mass spectra are complex as judged by eye, and there is little obvious difference between them. One way of highlighting any differences between these spectra is simply to subtract one from the other; subtraction spectra of this type (data not shown) indeed show that the intensities of some masses are significantly different (typically in the range $\pm$1% total ion count). The next stage is, therefore, to ascertain if these differences due to instrument drift are large enough to be problematic in using neural networks trained with data from time 1 to give accurate estimates of the amount of lysozyme from pyrolysis mass spectra collected at time 2.

Data collected from time 1 from mixing lysozyme in glycogen were split into two sets. The training set contained the normalized triplicate ion intensities from the pyrolysis mass spectra from 0, 10, 20, 30, 40, 50, 60, 70, 80, 90, and 100 μg of lysozyme in 20 μg of glycogen, while the cross-validation set contained both the training set and the 10 "unknown" pyrolysis mass spectra (5, 15, 25, 35, 45, 55, 65, 75, 85, and 95 μg of the determinand lysozyme in 20 μg of glycogen). We then trained ANNs, using the standard back-propagation algorithm, with the normalized PyMS data from the training sets as the inputs and the amount of determinand (0−100 μg of lysozyme) mixed in 20 μg of glycogen as the output. The details of input and output scaling and the length of training are given in Table 2; these were previously found to give optimal neural network solutions.[38] Once trained to 0.5% RMS error in the training set, the ANN was interrogated with the training and cross-validation sets, and a plot of the network's estimate versus the true amount of lysozyme in 20 μg of glycogen (Figure 2) gave a linear fit which was indistinguishable from the expected proportional fit (i.e., $y = x$). It was therefore evident that the network's estimate of the quantity of lysozyme in the mixtures was very similar to the true quantity, both for spectra that were used as the training set (○) and, more importantly, for the "unknown" pyrolysis mass spectra (□).

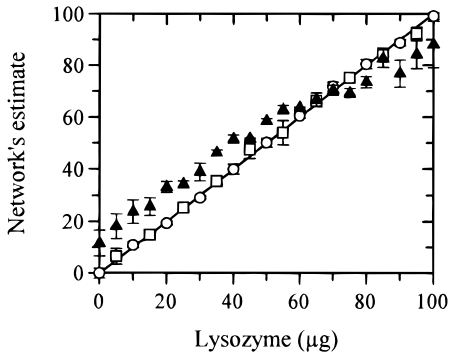

Figure 2. Estimates of trained 150-8-1 neural networks versus the true amount of lysozyme (0−100 μg in 20 μg of glycogen) for data collected at time 1 (27 August, 1992; ○, training set; □, cross-validation set) and time 2 (19 April, 1994; ▲, PyMS data). Networks were trained with PyMS data from time 1 using the standard back-propagation algorithm to 0.5% RMS error. Data points are the averages of the quadruplicate pyrolysis mass spectra, and the error bars show standard deviation. The solid line is the expected proportional fit.

Once the neural network was optimally trained (i.e., trained to give the best generalization as judged by the cross-validation set), the next stage was to interrogate the network with all the

Table 3. Comparison of a Trained Neural Network with Mass Spectral Data from Time 1 Interrogated with New Data from Time 2 and the Same Data after Drift Correction Using Either Neural Networks or Linear Transformations

	time 1	time 2	ANN correction		linear transformation[a]	
			150-8-150	150-150	method 1	method 2
Quantification of Lysozyme in Glycogen						
error (%)	0.83	8.68	3.49	2.77	10.30	6.29
slope	0.99	0.73	0.94	0.93	0.62	0.77
intercept	0.67	17.21	4.88	4.18	14.44	8.72
correln coeff	1.00	0.99	0.99	1.00	0.99	0.99
Quantification of Ampicillin in *E. coli*						
error (%)	1.70	64.76	3.69	3.19	7.33	5.50
slope	0.99	0.56	1.00	1.03	1.13	0.87
intercept	35.30	−2142.40	69.40	−31.08	−127.00	400.84
correln coeff	1.00	0.99	0.99	0.99	0.98	0.98
Quantification of *S. aureus* in *E. coli*						
error (%)	1.24	16.83	3.41	5.06	7.47	7.67
slope	1.03	0.87	1.01	1.05	1.09	0.99
intercept	−1.43	23.06	1.38	−2.97	−3.39	5.54
correln coeff	1.00	0.95	0.99	0.99	0.98	0.97

[a] Linear transformations for a mass-by-mass correction were carried out as described in the text. Method 1 corrected using linear subtractions, (new mass) − [average of (new calibration mass−old calibration mass)]; method 2 corrected using linear ratios, (new mass)[average ratio of (old calibration mass/new calibration mass)].

normalized pyrolysis mass spectra of 0−100 μg of lysozyme (in steps of 5 μg) in 20 μg of glycogen collected at time 2. The network's estimate for these samples is also shown in Figure 2 (▲), where it can be seen that the network's estimate versus the true amount of lysozyme in 20 μg of glycogen no longer gave a truly linear (or proportional) fit. The percentage error in these estimates (Table 3) was 8.68%, compared to 0.83% for the same samples analyzed at time 1. Table 3 also shows the slope and intercept of the best-fit line for the network's estimates versus the true concentrations. It is notable that the slope for data collected at time 1 was 0.99, but it was only 0.73 for those collected at time 2. These results clearly show that the pyrolysis mass spectra of the same material had changed significantly between 27 August, 1992 (time 1) and 19 April, 1994 (time 2), thus resulting in an inability to use neural networks trained with data collected at time 1 to give accurate predictions for data from the same material subsequently collected at time 2.

It is therefore necessary to apply a mathematical correction procedure to compare directly two sets of data of the same material. As described in the Experimental Section, calibration spectra (standards) were chosen at the two time periods, and these were the triplicate normalized pyrolysis mass spectra containing 0, 25, 50, 75, and 100 μg of lysozyme in 20 μg of glycogen. These standards were used in each of the four numerical methods also described above, two of which were based on neural networks and two on linear transformations.

After training 150-8-150 neural networks to transform new mass spectra collected at time 2 into those previously collected at time 1, the first stage was to observe how similar the transformed mass spectra were to the old mass spectra of the same material. Figure 1 shows the normalized pyrolysis mass spectra of 35 μg of lysozyme mixed with 20 μg of glycogen (chosen because it had not been used to train the neural network) analyzed on 27 August, 1992 (time 1, —), 19 April, 1994 (time 2, – –), and the spectra

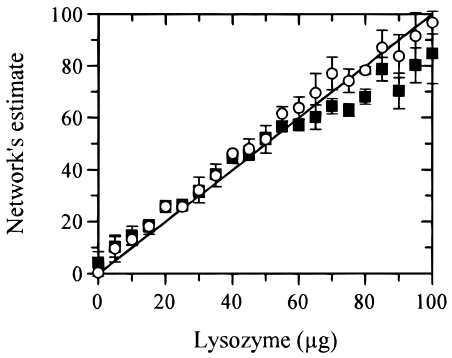

Figure 3. Estimates of trained 150-8-1 neural networks versus the true amount of lysozyme (0−100 μg in 20 μg of glycogen) for data collected at time 2 (19 April, 1994; ■, linear transformation; ○, neural network transformation) after correction for instrumental drift. Networks were trained with PyMS data from time 1 using the standard back-propagation algorithm to 0.5% RMS error. Data points are the averages of the triplicate pyrolysis mass spectra, and the error bars show standard deviation. The solid line is the expected proportional fit.

from time 2 transformed by a 150-8-150 neural network (- - -). It is clear that there is, as expected from subtraction spectra (data not shown) and Figure 2, some difference in the mass spectra collected at the two different time, but that the transformed spectrum shows little or no difference compared to the real mass spectra collected at time 1; it was therefore evident that this correction procedure had, indeed, corrected for instrumental drift.

The next stage was to use these neural network transformed spectra, and those transformed by linear methods, to challenge neural networks trained with PyMS data from time 1 to quantify the amount of lysozyme in mixtures with 20 μg of glycogen. These ANNs employed the standard back-propagation algorithm and were trained to 0.5% RMS error as detailed in Table 2. Figure 3 shows the estimates of trained 150-8-1 neural networks versus the true amount of lysozyme (0−100 μg in 20 μg of glycogen) for data collected at time 2 (19 April, 1994) after correction for instrumental drift by either (a) 150-8-150 ANN drift correction (○) or (b) a linear mass-by-mass subtraction correction (■). It can clearly be seen that the neural network transformed mass spectra give better estimates than do the linear transformed spectra; this is particularly notable within the range 50−100 μg of lysozyme. The error in the estimates and the slope and intercept of the best-fit lines for these and the other two correction methods used are detailed in Table 3. The typical error in the neural network-based transformations was 3.49% for the 150-8-150 ANN and slightly lower, 2.77%, for the neural network with no hidden layer, compared with 8.68% for no correction applied; for the linear subtraction and linear ratios on the individual m/z intensities, the errors were 10.30% and 6.29%, respectively. It is likely that using the ratios to correct was better than using subtractions of drift because the latter will introduce some negative m/z intensities in the transformed spectra; this phenomenon is not possible with real data and is, in this instance, a consequence of having to normalize to percentage total ion count.

Further to highlight the success of the neural network corrections over the linear ones, the transformed mass spectra were analyzed with the data collected at time 1 and time 2 by PCA (data not shown). In both of these plots, the first principal component describes the features in the mass spectra which account for the increasing amount of lysozyme, and the second

principal component accounts for the effect of instrument drift. It can be seen (data not shown) that both transformations "move" the time 2 data closer to time 1 but that the neural network transformation is more successful because the line from these transformed data more closely overlaps the line from the data collected at time 1. Furthermore, the line from time 2 contains a curvature in the 50−80 μg lysozyme region which is straightened out when transformed using the 150-8-150 ANN; this curvature remains when the mass spectra are linearly altered, and this may explain why the estimates using the linear transformed spectra were poor in the range 50−100 μg of lysozyme (Figure 3).

In conclusion, neural networks can be trained with pyrolysis mass spectral data to quantify lysozyme in glycogen; however, these neural network models cannot be used with mass spectra from identical material collected 600 days later. The 150-8-150 and 150-150 neural networks can be used to correct successfully for the drift observed in these pyrolysis mass spectra, so that neural network models created using old data (time 1) can be used with newly acquired spectra from time 2. It is likely that this success was due to the ability of ANNs to map nonlinearities as well as linearities, since linear transformation methods alone could not be used to correct for instrument drift.

(ii) Quantification of Ampicillin in *E. coli*. Data collected from time 1 from mixing ampicillin with *E. coli* were split into two sets. The training set contained the normalized triplicate ion intensities from the pyrolysis mass spectra from 0, 500, 1000, 1500, 2000, 2500, 3000, 3500, 4000, 4500, and 5000 μg mL^{-1} of ampicillin mixed with 40 mg mL^{-1} *E. coli*, while the cross-validation set contained both the training set and the 10 "unknown" pyrolysis mass spectra (250, 750, 1250, 1750, 2250, 2750, 3250, 3750, 4250, and 4750 μg mL^{-1} of the determinand ampicillin in 40 mg mL^{-1} *E. coli*). We then trained ANNs, using the standard back-propagation algorithm, with the normalized PyMS data from the training sets as the inputs and the amount of determinand (0−5000 μg mL^{-1} ampicillin) mixed in 40 mg mL^{-1} *E. coli* as the output. The details of input and output scaling and the length of training are given in Table 2; these were previously found to give optimal neural network solutions.[40] Once trained to 1.0% RMS error in the training set, the ANN was then interrogated with the training and cross-validation sets, and a plot of the network's estimate versus the true concentration of ampicillin in *E. coli* (Figure 4) gave a linear fit which was indistinguishable from the expected proportional fit. It was therefore evident that the network's estimate of the ampicillin titer in the mixtures was very similar to the true quantity, both for spectra that were used as the training set (○) and, more importantly, for the "unknown" pyrolysis mass spectra (□).

Once the neural network was optimally trained, the next stage was to interrogate the network with all the normalized pyrolysis mass spectra of 0−5000 μg mL^{-1} ampicillin (in steps of 250 μg mL^{-1}) in 40 mg mL^{-1} *E. coli* collected at time 2. The network's estimate for these samples is also shown in Figure 4 (▲), where it can be seen that the network's estimate versus the true ampicillin titer was very inaccurate. The percentage error in these estimates (Table 3) was 64.76% compared to 1.70% for the same samples analyzed at time 1. These results unequivocally show that the pyrolysis mass spectra of the same material had changed significantly between 22 July, 1993 (time 1) and 19 April, 1994 (time 2), thus resulting in an inability to use neural networks trained with data collected at time 1 to give predictions for data from the same material subsequently collected at time 2.

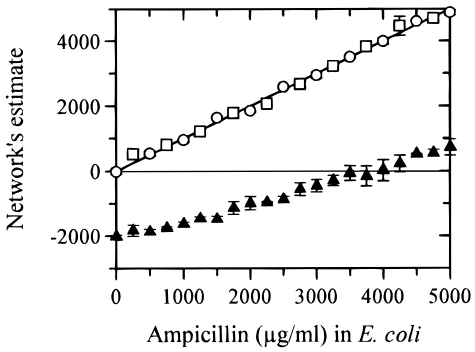

Figure 4. Estimates of trained 150-8-1 neural networks versus the true ampicillin titer (0−5000 μg mL^{-1} in 40 mg mL^{-1} *E. coli*) for data collected at time 1 (22 July, 1993; ○, training set; □, cross-validation set) and time 2 (19 April, 1994; ▲, PyMS data). Networks were trained with PyMS data from time 1 using the standard back-propagation algorithm to 1.0% RMS error. Data points are the averages of the triplicate pyrolysis mass spectra, and the error bars show standard deviation. The solid line is the expected proportional fit.

It is therefore necessary to apply a mathematical correction procedure to compare directly these two sets of data. As described in the Experimental Section, calibration spectra (standards) were chosen at the two time periods, and these were the triplicate normalized pyrolysis mass spectra containing 0, 1250, 2500, 3750, and 5000 μg mL^{-1} ampicillin in 40 mg mL^{-1} *E. coli*. These standards were used in each of the four numerical methods described above and were used to transform the mass spectra collected at time 2.

The first stage was to observe the natural relationships between the transformed data using neural networks without a hidden layer in this example (150-150 architecture) and the linear mass-by-mass ratio transformed data with data collected on 22 July, 1993 (time 1) and 19 April, 1994 (time 2) using PCA (Figure 5). Figure 5a shows the effect on transforming data from time 2 to time 1 using the linear ratio method, and Figure 5b shows the effect of a 150-150 ANN transformation. In both plots, the first principal component seems to relate to the effect of instrument drift, while the second principal component is controlled by the features in the mass spectra which account for the increasing ampicillin titer. As observed previously, both transformations "move" the time 2 data closer to the time 1 data, but the neural network transformation is more successful because the line from these transformed data (Figure 5b) overlaps the line from the data collected at time 1 more. It is particularly noteworthy that the linear transformed estimates are parallel with the time 2 untransformed data (Figure 5a), whereas a 150-150 transformation produces data which map accurately onto the data from time 1 (Figure 5b); this may again be explained by the ability of the ratio transformation to correct the mass spectra only in a linear manner.

The next stage was to use these 150-150 neural network transformed spectra and those transformed by the linear ratio method to challenge neural networks trained with PyMS data from time 1 to assess the ampicillin titer when mixed with 40 mg mL^{-1} *E. coli*. These ANNs employed the standard back-propagation algorithm and were trained to 1.0% RMS error as detailed in Table 2. Figure 6 shows the estimates of trained 150-8-1 neural networks versus the true ampicillin concentration (0−5000 μg mL^{-1}) for data collected at time 2 (19 April, 1994) after correction for instrumental drift by either (a) 150-150 ANN drift correction (○) or (b) a linear mass-by-mass ratio correction (■). It can be

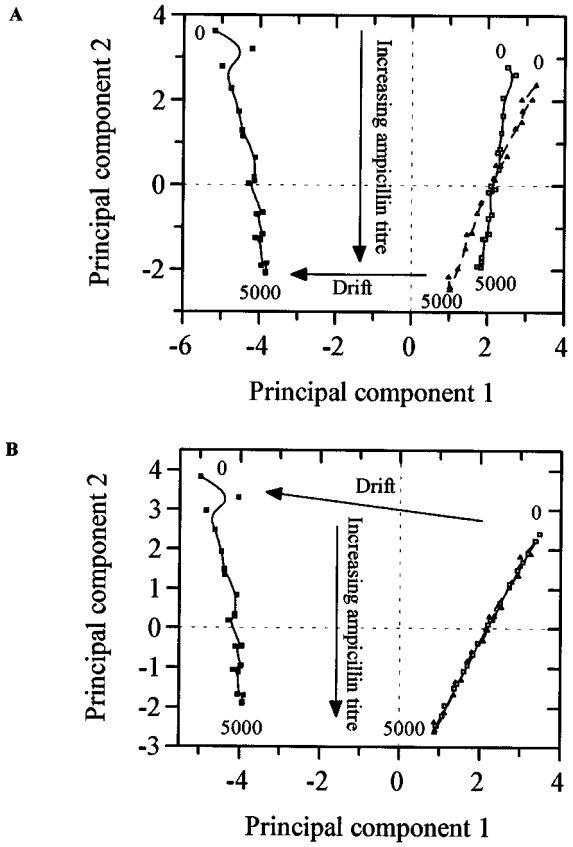

Figure 5. Principal components analyzes plots based on the PyMS data for 0−5000 μg mL^{-1} lysozyme mixed with 40 mg mL^{-1} *E. coli* for data collected on 22 July, 1993 (time 1, ▲) and 19 April, 1994 (time 2, ■) compared with (□) either a linear mass-by-mass ratio correction (A) or a 150-150 neural network (B) drift correction of the mass spectra collected at time 2 transformed into those collected at time 1. The first two principal components (PCs) accounted for 76% and 22% (98% total) of the total variance in plot A and 77% and 22% (99% total) in plot B. In both plots, the first PC accounts for the effect of instrument drift, and the second PC describes the features in the mass spectra which account for the increasing ampicillin titer.

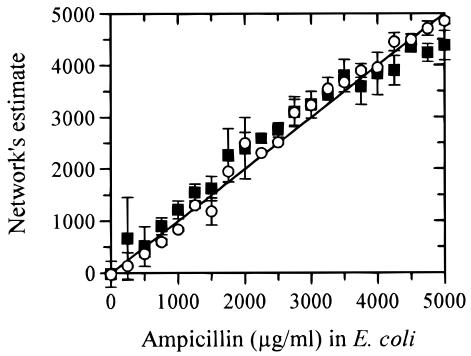

Figure 6. Estimates of trained 150-8-1 neural networks *vs.* the true ampicillin titer (0−5000 μg mL^{-1} in 40 mg mL^{-1} *E. coli*) for data collected at time 2 (19 April, 1994; ■, linear transformation; ○, neural network transformation) after correction for instrumental drift. Networks were trained with PyMS data from time 1 using the standard back-propagation algorithm to 1.0% RMS error. Data points are the averages of the triplicate pyrolysis mass spectra, and the error bars show standard deviation. The solid line is the expected proportional fit.

observed that the neural network-transformed mass spectra give better estimates than do the linear transformed spectra. The error in the estimates and the slope and intercept of the best-fit lines for these and the other two correction methods used are detailed in Table 3. The typical error in the neural network-based transformations was 3.19% for the 150-150 ANN and 3.69% for the neural network with eight nodes in the hidden layer, compared with 64.76% for no correction applied. Again ANNs with no hidden layer gave slightly better estimates than did those containing a hidden layer. For the linear subtraction and linear ratios on the individual *m/z* intensities, the errors were 7.33% and 5.50%, respectively. In this example, the linear methods appear to have performed rather well; however, the slopes of the best-fit lines of the estimates versus the known ampicillin titer (Table 3) were 1.13 and 0.87 for the linear subtraction and ratio correction methods, compared to 1.00 and 1.03 for the 150-8-150 and 150-150 ANN corrections, respectively.

In conclusion, neural networks can be trained with pyrolysis mass spectral data to quantify ampicillin in *E. coli*, as a model of mixtures containing a biological cell suspension and a product metabolite of interest. These neural network models can not however be used with mass spectra from identical material collected 271 days later. The 150-8-150 and 150-150 neural networks can be used to correct successfully for the drift observed in these pyrolysis mass spectra, so that neural network models created using old data from time 1 can be used with newly acquired spectra from time 2.

(iii) Quantification of *S. aureus* in *E. coli*. Data collected from time 1 from mixing *S. aureus* with *E. coli* were split into two sets. The training set contained the normalized triplicate ion intensities from the pyrolysis mass spectra from 0, 25, 50, 75, and 100% *S. aureus* mixed with *E. coli*, while the cross-validation set contained both the training set and the eight "unknown" pyrolysis mass spectra (10, 20, 30, 40, 60, 70, 80, and 90%). ANNs were then trained, using the standard back-propagation algorithm, with the normalized PyMS data from the training sets as the inputs and the percentage *S. aureus* mixed with *E. coli* as the output. The details of input and output scaling and the length of training are given in Table 2; these were previously found to give optimal neural network solutions.[25] This 150-8-1 neural network was optimally trained (i.e., trained to give the best generalization as judged by the cross-validation set) to 0.3% RMS error in the training set. The ANN was then interrogated with the training and cross-validation sets from time 1, the new pyrolysis mass spectra from time 2, and these data after instrument drift correction by each of the four transformation methods.

The percentage error in these estimates and the slopes, and intercepts of the best-fit lines of the estimates versus the *S. aureus* content are given in Table 3. It can be seen that, on the day, error (as judged by the estimates from time 1) was only 1.24%, and when interrogated with spectra collected 535 days later, it was 16.83%. The errors in the estimates after correction using 150-8-150 and 150-150 ANNs were 3.41% and 5.06%, so in this example the neural network containing a hidden layer was better for correcting for instrumental drift; for the linear subtraction and linear ratio transformation methods the errors, although similar, were less good, calculated to be 7.47% and 7.67%.

In conclusion, neural networks can be trained with pyrolysis mass spectral data to quantify a mixed population of *S. aureus* and *E. coli*. However, these neural network models cannot be used to give accurate *S. aureus* content estimates for mass spectra from identical material collected 535 days later. The 150-8-150 and 150-150 neural networks can be used to correct successfully for instrumental drift so that neural network models created using

Table 4. Identities of the Bacteria in the Test Set and Training Set from Time 1 as Judged by a Neural Network Trained with Mass Spectral Data from Time 1, Compared with New Data from Time 2 and Those Data after Drift Correction Using Either 150-8-150 Neural Network or Linear Mass-by-Mass Ratio Transformation

	results from PyMS data						results after correcting for drift					
	time 1			time 2			150-8-150 ANN			linear mass-by-mass ratio transformation		
identity	a	b	c	a	b	c	a	b	c	a	b	c
a[a]	1.0	0.0	0.0	1.0	0.0	0.0	1.0	0.0	0.0	1.0	0.0	0.0
a	1.0	0.0	0.0	1.0	0.0	0.0	0.7	0.3	0.0	1.0	0.0	0.0
a	1.0	0.0	0.0	1.0	0.0	0.0	0.7	0.3	0.0	1.0	0.0	0.0
a	1.0	0.0	0.0	1.0	0.0	0.0	1.0	0.0	0.0	1.0	0.0	0.0
a	1.0	0.0	0.0	1.0	0.0	0.0	1.0	0.0	0.0	1.0	0.0	0.0
a	1.0	0.0	0.0	1.0	0.0	0.0	0.7	0.3	0.0	1.0	0.0	0.0
a[a]	1.0	0.0	0.0	1.0	0.0	0.0	1.0	0.0	0.0	0.8	0.0	0.0
a	1.0	0.0	0.0	1.0	0.0	0.0	0.7	0.3	0.0	1.0	0.0	0.0
a	1.0	0.0	0.0	1.0	0.0	0.0	0.8	0.1	0.0	1.0	0.0	0.0
b[a]	0.0	1.0	0.0	*0.8*	*0.7*	*0.0*	0.0	1.0	0.0	0.0	0.9	0.0
b	0.1	1.0	0.0	*1.0*	*0.5*	*0.0*	0.0	1.0	0.0	0.2	0.8	0.0
b[a]	0.0	1.0	0.0	*1.0*	*0.4*	*0.0*	0.0	1.0	0.0	0.3	0.8	0.0
b	0.0	1.0	0.0	0.3	0.8	0.0	0.0	0.7	0.3	0.0	0.9	0.0
b	0.2	0.9	0.0	*1.0*	*0.2*	*0.0*	*0.7*	*0.4*	*0.0*	*0.6*	*0.5*	*0.0*
c[a]	0.0	0.0	1.0	*0.0*	*0.9*	*0.3*	0.0	0.0	1.0	0.0	0.0	1.0
c	0.0	0.0	1.0	*0.0*	*0.9*	*0.3*	0.0	0.0	1.0	0.0	0.0	1.0
c[a]	0.0	0.0	1.0	0.0	0.1	1.0	0.0	0.0	1.0	0.0	0.0	1.0
c	0.0	0.0	1.0	0.0	0.0	1.0	0.0	0.0	1.0	0.0	0.0	1.0
c	0.0	0.0	1.0	0.0	0.3	0.9	0.1	0.0	0.7	0.0	0.0	1.0
misidentified	0/19 (0%)			6/19 (31.6%)			1/19 (5.3%)			1/19 (5.3%)		

[a] Results from the pyrolysis mass spectra from the time 1 training set. These spectra were also chosen as the calibration samples for drift correction. Values in italics are those *P. acnes* isolates which were misidentified.

old data from time 1 can be used to give accurate *S. aureus* measurements from newly acquired spectra.

(iv) Identification of *P. acnes*. Data collected from time 1 from the 19 strains of *P. acnes* were split into two sets. The training set contained the normalized triplicate ion intensities from the pyrolysis mass spectra from two isolates from each of the people (details are given in Table 4), and the three outputs were binary encoded as explained above. The interrogation set contained the triplicates of all 19 pyrolysis mass spectra. The 150-8-3 ANNs were then trained, using the standard back-propagation algorithm, with the normalized PyMS data from the training sets as the inputs and the bacterial identity as the output. The details of input and output scaling are given above. Training was stopped when the %RMS error in the training set was 1%, this took approximately 2×10^3 epochs. After training, the interrogation set from time 1 was applied to the input nodes of the neural network, and the answers are given in Table 4, where it can be seen that each of the 19 bacteria was identified correctly.

Once the neural network was trained to give correct results for "unknown" pyrolysis mass spectra, the next stage was to interrogate with all the normalized pyrolysis mass spectra from the same bacteria collected 125 days later at time 2. The network's identities for these samples are also shown in Table 4, where it can be seen that 6 of the 19 bacteria were incorrectly identified. These results show unequivocally that the pyrolysis mass spectra of the same material had changed significantly between 28 January, 1994 (time 1) and 2 June, 1994 (time 2), thus resulting in an inability to use neural networks trained with data collected at time 1 (to identify these *P. acnes* strains) to give accurate identities for data from the same bacteria subsequently collected at time 2.

It is therefore necessary to apply a mathematical correction procedure to compare directly these two sets of data. Calibration spectra were chosen at the two time periods, and these were the triplicate normalized pyrolysis mass spectra from two isolates from each of the three people; details are given in Table 4. These standards were used by each of the four numerical methods described above and were used to transform the mass spectra collected at time 2.

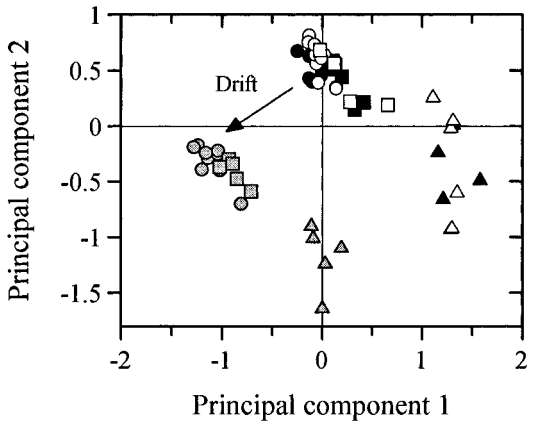

Figure 7. Principal components analysis plot based on the PyMS data for the *P. acnes* human isolates for data collected on 28 Jan, 1994 (time 1, solid symbols) and 2 June, 1994 (time 2, shaded symbols) compared with a 150-8-150 neural network drift correction (open symbols) of the mass spectra collected at time 2 transformed into those collected at time 1. The first two principal components (PCs) accounted for 54% and 33% (87% total) of the total variance. A combination of the first and second PCs can be seen to describe the effects of instrument drift. Circles, bacterial isolates from person a; squares, from person b; and triangles, from person c.

The first stage was to carry out PCA to observe the natural relationships between the transformed data using 150-8-150 neural networks with data collected at time 1 and time 2; the PCA plot is shown in Figure 7, where it can be observed that a combination

of the first two principal components clearly reflects the effect of instrument drift (indicated by the arrow). In this PCA plot, it can seen that the isolates from person c form a distinct cluster (triangles) and that, although the isolates from person a (circles) and person b (squares) cluster tightly together, they can be separated. This may help to explain why the neural network trained with data from time 1 when interrogated with new pyrolysis mass spectra, misidentified four of the five isolates from person b as being from person a. The most important observation from this PCA plot is that the 150-8-150 ANN-transformed mass spectra (open symbols) overlap with the data collected at time 1 (closed symbols) and no longer cluster with the data from time 2 (shaded symbols). Moreover, the strains from each of the three people can be seen to cluster together.

The next stage was to use these neural network-transformed spectra, and those transformed by the linear ratio method, to challenge the 150-8-3 neural networks trained with PyMS data from time 1 to identify the three *P. acnes* strains. The results after interrogation are shown in Table 4, where instead of misidentifying 6 of the 19 bacteria (31.6% of total), only one isolate (5.3% of total) from person b was misidentified; the same bacterium was identified incorrectly by both of these methods. When the other two correction techniques (150-150 ANNs and linear subtraction method) were used to transform the pyrolysis mass spectra and to challenge the 150-8-3 neural network, the same results were seen; 18 of the 19 bacteria were identified correctly, as opposed to only 13, and the same strain from person b was misclassified.

In conclusion, neural networks can be trained with pyrolysis mass spectral data to identify *P. acnes* isolated from the foreheads of three individuals. However, these neural network models cannot be used to give accurate classifications for mass spectra from the same bacteria collected 125 days later. The 150-8-150 and 150-150 neural networks and the two linear models were used to correct successfully for instrumental drift, so that neural network models created using old data from time 1 can be used to give accurate isolate identities from newly acquired spectra. It is noteworthy that these isolates were of the same species of *Propionibacterium* and so were phenotypically very similar; that these transformation procedures were sensitive enough to corrected for drift was, therefore, very encouraging. Although in this example, all methods could be used to correct for drift, the results from the other three examples indicate strongly that the prefered method for instrumental drift correction would employ ANNs, since they have the ability to perform nonlinear mappings in addition to linear ones.

CONCLUSIONS

We have shown here and elsewhere[25,38,40] that pyrolysis mass spectrometry and neural networks can be used to accurately quantify binary mixtures of lysozyme in glycogen, *S. aureus* mixed with *E. coli*, and ampicillin in *E. coli*. ANNs can also be applied to PyMS data to identify correctly human isolates of *P. acnes* isolated from the foreheads of three individuals. However, when identical materials were analyzed by PyMS at later dates, the neural network models could not be used to give accurate determinand estimates or bacterial identities. It was therefore evident that this lack of long-term reproducibility was due to instrument drift.

For PyMS to be used either for the routine identification of microorganisms or to quantify biological systems, it is paramount that newly acquired spectra be compared to those previously collected. To correct for the instrumental drift observed, four methods were exploited which attempted to transform new spectra into old spectra, using a set of calibration samples, or standards, which had been analyzed at both times (time 1, old data; time 2, new data). Two methods relied on linear corrections alone either by subtracting the drift seen in each mass or by applying a weighting to each new mass based on the average ratio of old calibration mass to new calibration mass. The use of linear correction techniques does, however, assume that the drift is uniform (i.e., linear) with time, which is obviously not the case; therefore two other methods which exploited neural networks were used. ANNs can carry out nonlinear as well as linear mappings from the input to the output nodes; in addition, they are purported to be robust to noisy data which are often associated with pyrolysis mass spectra.[38] In these models, the inputs to the ANNs were the new calibration masses and the outputs were the calibration masses, from the old spectra. Some ANNs contained a hidden layer of 8 nodes and had an architecture of 150-8-150, whereas some lacked a hidden layer and had a 150-150 topology.

In each of the three quantification examples, the neural network transformation techniques gave better corrections for drift. This can be determined by observing the lower errors between determinand estimates and known titers seen in Table 3 and by examining PCA plots of old, new, and transformed mass spectra (Figure 5). Furthermore, whether the ANN contained a hidden layer or not made very little difference to the transformations seen. For the identification of human *P. acnes* isolates, all four methods corrected for instrument drift and correctly identified 18 of the 19 isolates; before correction, 6 bacteria were misidentified. However, given that ANNs gave better drift corrections than did the linear transformations for the other examples, it would be advisable to use ANNs to correct for drift.

In conclusion, neural networks can be used successfully to correct for instrumental drift so that neural network models created using old, previously collected data can be employed to give accurate estimates of determinand concentration or bacterial identities (or, indeed, other materials) from newly acquired spectra when calibrated with standards common to the two data sets.

It should seem obvious that this approach is not limited to pyrolysis mass spectrometry but is generally applicable to any analytical tool which is prone to instrumental drift (which cannot be compensated for by tuning), such as infrared spectroscopy, nuclear magnetic resonance, and gas chromatography, as well as other forms of mass spectrometry.

ACKNOWLEDGMENT

R.G. is funded as a research fellow by the Wellcome Trust (Grant No. 042615/Z/94/Z). D.B.K. thanks the Chemicals & Pharmaceuticals Directorate of the UK BBSRC for financial support under the terms of the LINK scheme in Biochemical Engineering, in collaboration with Horizon Instruments, Neural Computer Sciences, and Zeneca Bioproducts plc.

Received for review July 6, 1995. Accepted November 7, 1995.[⊗]

AC950671T

[⊗] Abstract published in *Advance ACS Abstracts,* December 15, 1995.